

Hyperfine structure in the red emission system of NbN

J.-L. Femenias,* C. Athenour,* and T. M. Dunn

Chemistry Department, University of Michigan, Ann Arbor, Michigan 48104
(Received 16 January 1974)

A detailed study of hyperfine structure observed in the 0,0 band of the ${}^3\Phi(a_g) \rightarrow {}^3\Delta(a_g)$ system of NbN has shown that the secondary hyperfine effects observed in this structure are not due to a perturbation in the ${}^3\Delta$ state but rather to the presence of a nonnegligible hyperfine effect in the ${}^3\Phi$ excited state. Calculations of the intensity factors corresponding to the observed transitions confirm this hypothesis and give results in excellent agreement with experiment.

I. INTRODUCTION

During the past few years, many nuclear hyperfine effects due to coupling between nuclear spins and various molecular angular momenta have been observed in the electronic spectra of diatomic molecules. For the most part, the various coupling cases discussed by Frosch and Foley¹ in 1952, have now actually been observed. Case a_g has been observed in the $A_1 {}^2\Pi_{1/2}$ state of HgH^{2,3} which shows an unusual Λ doubling effect due to terms which are off diagonal in Λ , in the hyperfine Hamiltonian, and in the ${}^3\Pi$ state of BiH,^{4,5} where case c tendencies are undoubtedly present. Examples of b_{gJ} are the $X^2\Sigma$ state of HgH,^{2,3} and the $B^2\Sigma$ state of CN,⁶⁻⁸ while case c_g has been observed in various systems of BiO.^{9,10}

More importantly, it has been found that the ground electronic states of diatomic oxides and nitrides of the transition metals involve an s electron, almost completely localized on the metal atom,¹³ and this has resulted in many excellent examples of large nuclear hyperfine effects in the electronic transitions of these molecules. This is the case for the ${}^4\Sigma^-$ (ground) states of VO^{11,12} and NbO,⁵ where the coupling case is b_{gJ} , while the ${}^2\Sigma$ (ground) states of ScO,^{13,14} LuO,¹⁵ and LaO¹⁶ have exhibited b_{gS} coupling with b_{gJ} tendencies having been demonstrated for the high N levels of LaO.¹⁶

Discovery of the ${}^3\Phi \rightarrow {}^3\Delta$ system of NbN by Dunn and Rao¹⁷ in 1969, added this unusual example to the others. It was observed that there is a very large hyperfine splitting at low values of J (and inversely proportional to J^2), which allowed them to conclude that the ${}^3\Delta$ state is an excellent example of case a_g coupling. As well as the main hyperfine effects, there are secondary splittings. These, together with the role of NbN as the first nonhydride molecule to exhibit a_g coupling, seemed to us to call for a thorough analysis of all the observed hyperfine effects—both primary and secondary.

II. THE SPECTRUM OF NbN

The main interest in this spectrum is in the very large hyperfine effects observed in the low J members of the R branches in the ${}^3\Phi_4 \rightarrow {}^3\Delta_3$ and ${}^3\Phi_2 \rightarrow {}^3\Delta_1$ subbands of the 0,0 band (see Fig. 1). No such effects were observed in the ${}^3\Phi_3 \rightarrow {}^3\Delta_2$ subband (other than a slightly larger than normal linewidth of the $R(2)$ line); a possible explanation of this was provided by the original authors. The principal component of the hyperfine effect can be attributed to the presence of a large component of "s"

electronic character, so that there is an appreciable electron density close to the niobium atom nucleus in the ${}^3\Delta$ state. The interaction between electron and nuclear spins in this case places great importance on the "Fermi term" ($bI \cdot S$) in the Frosch and Foley Hamiltonian.¹ In this hypothesis, all of the hyperfine effect is confined to the ${}^3\Delta$ state in case a_g according to the hyperfine Hamiltonian^{1,5}:

$$H_{\text{hfs}} = [a\Lambda + (b+c)\Sigma][\Omega/J(J+1)] \mathbf{I} \cdot \mathbf{J}, \text{ with } \mathbf{I} + \mathbf{J} = \mathbf{F}. \quad (1)$$

In the situation where $a \sim 0$, the presence of the term Ω leads to the expectation that there will be a factor of ~ 3 in the linewidths of lines with the same value of J in the two subbands ${}^3\Phi_4 \rightarrow {}^3\Delta_3$ and ${}^3\Phi_2 \rightarrow {}^3\Delta_1$. Experimentally, the value is somewhat less than this (~ 1.6).

Still with the condition $a \sim 0$, the formula shows that no hyperfine splitting is possible when $\Sigma = 0$, i. e., for the ${}^3\Phi_3 \rightarrow {}^3\Delta_2$ subband. For this reason, the small increased linewidth observed for $R(2)$ was attributed to case c tendencies of the ${}^3\Delta$ state and this is, to some extent, supported¹⁸ by the inequality of the distances between the subbands ${}^3\Phi_4 \rightarrow {}^3\Delta_3$ and ${}^3\Phi_3 \rightarrow {}^3\Delta_2$, compared with the distance from ${}^3\Phi_3 \rightarrow {}^3\Delta_2$ to ${}^3\Phi_2 \rightarrow {}^3\Delta_1$.

Despite a general understanding of the origin of the hyperfine structure, the presence of the "extra" components in the $R(1)$ and $R(2)$ lines of the subband ${}^3\Phi_2 \rightarrow {}^3\Delta_1$ and in the low J members of the ${}^3\Phi_4 \rightarrow {}^3\Delta_3$ subband, has never been satisfactorily explained. The study of these secondary effects has led us to improve our previous experimental techniques, obtaining the spectra at a greater reciprocal dispersion ($\sim 0.2\text{--}0.4 \text{ \AA}/\text{mm}$ ¹⁸ and better resolution than the original studies.¹⁷ The microdensitometer traces of the first R lines in all three 0,0 subbands is given in Fig. 1.

The first thing one observes in the $R(1)$ line of the ${}^3\Phi_2 \rightarrow {}^3\Delta_1$ is the completely resolved doubling of the first two hyperfine components (corresponding to $F_\Delta = \frac{7}{2}$ and $\frac{9}{2}$) and the large number of components in the following lines. Unfortunately, the lines $R(3)$ and $R(5)$ of the ${}^3\Phi_4 \rightarrow {}^3\Delta_3$ subband are masked by strong atomic lines, which we have not been able to eliminate, and this has deprived us of some valuable information.

As a result of this, together with the fact that the ratio of the linewidths in the ${}^3\Phi_4 \rightarrow {}^3\Delta_3$ and ${}^3\Phi_2 \rightarrow {}^3\Delta_1$ subbands is too low when compared with the theoretical value, it is necessary to examine the various possible theoretical models to explain all of the effects observed.

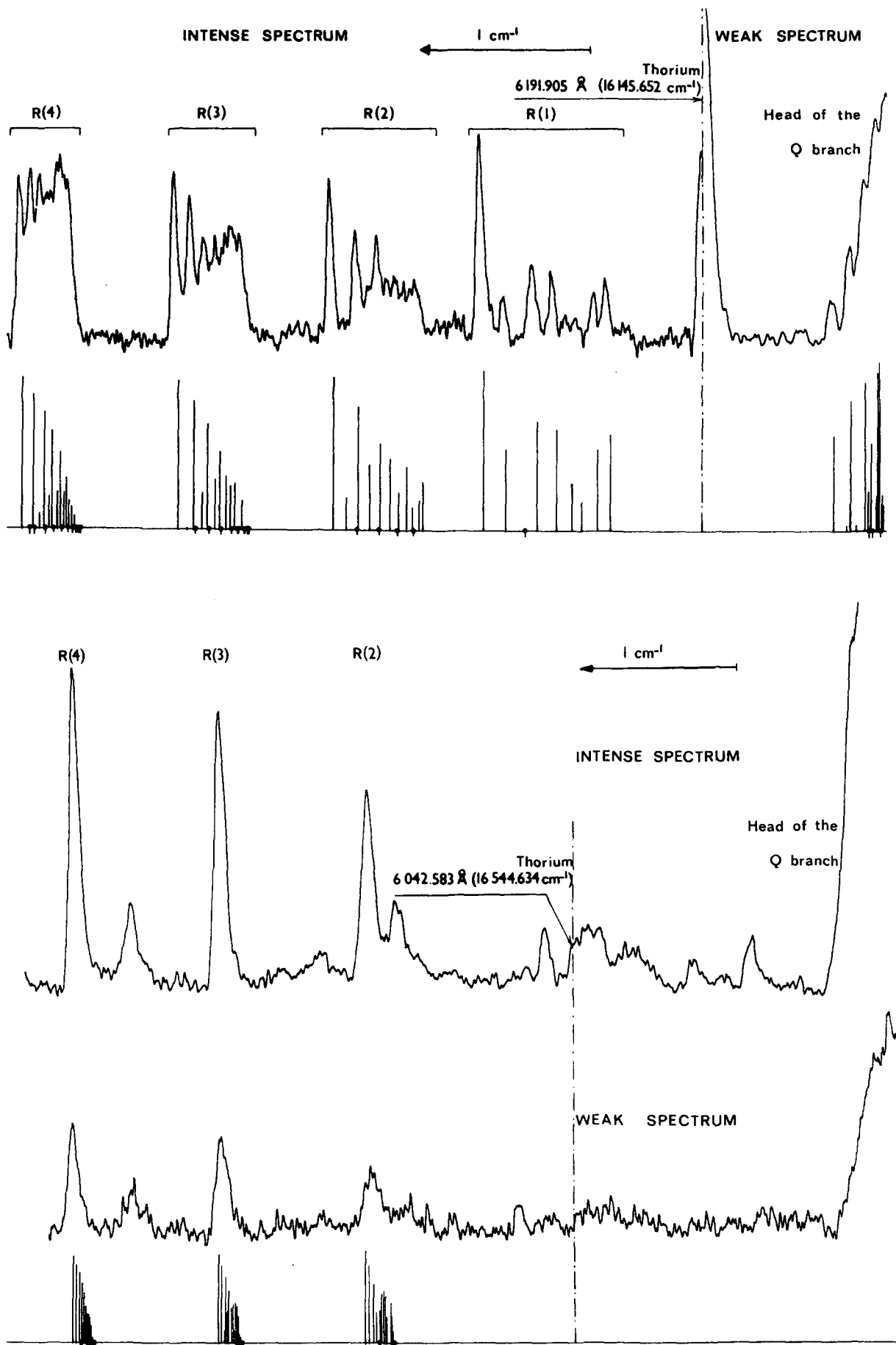


FIG. 1. Microdensitometer traces and theoretical structure of the spectrum using the hypothesis of a hyperfine effect in the ${}^3\Phi$ state. (For the significance of the intensities, see Ref. 25). (a) subband ${}^3\Phi_2 \rightarrow {}^3\Delta_1$, (b) subband ${}^3\Phi_3 \rightarrow {}^3\Delta_2$, (c) subband ${}^3\Phi_4 \rightarrow {}^3\Delta_3$.

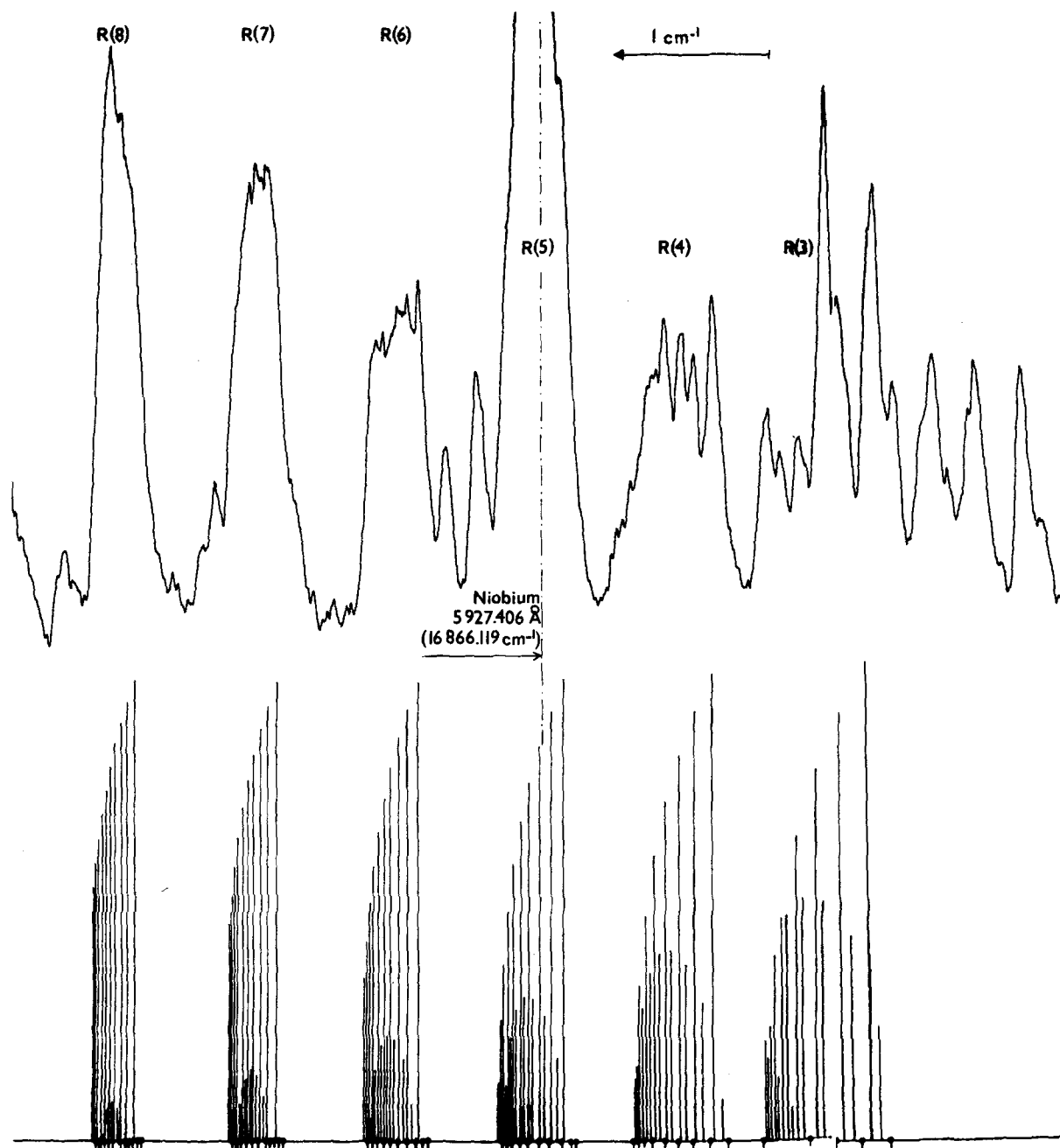


FIG. 1. (Continued)

III. THEORETICAL

We have discarded, *a priori*, certain hypotheses which are incompatible with the experimental observations. For example, a local Λ doubling in the ${}^3\Phi$ state which does not have the correct F dependence of the effect obtained in $R(1)$ of the ${}^3\Phi_2 \rightarrow {}^3\Delta_1$ subband and which only occurs in sixth order of perturbation theory. This seems excessive even for a localized perturbation and will not be discussed further. Thus, from such considerations, three possibilities have emerged and have been studied; the possibility of a tendency towards case a_α in the ${}^3\Delta$ state, the presence of a localized perturbation in the first levels of ${}^3\Delta_1$ thereby removing the Λ degeneracy and, finally, the existence of a nonnegligible

hyperfine interaction in the ${}^3\Phi$ state.

A. The a_α model

The observation of extra lines suggests the possibility of forbidden transitions ($\Delta J \neq 0, \pm 1$) due to the progressive transition of the ${}^3\Delta$ state from case a_α at low J to a_β at higher J . This was, therefore, studied as an intermediate coupling case in basis a_α by analogy with the well known treatments of Hund's coupling cases between a and b .¹⁹ If all interactions with other states, as well as interaction between the three substates of ${}^3\Delta$ are ignored, the Hamiltonian takes the following form:

$$H = H_{\nu\nu} + AL_z S_z + B(F^2 - F_z^2 + I^2 - I_z^2 + S^2 - S_z^2)$$

$$+ [aL_x + (b+c)S_x]I_x - B(F^+I_x + F^-I_x), \quad (2)$$

where H_{av} is the vibronic part, the notation F^* and I_x is defined elsewhere.²⁰ The other notation is normal. For each subsystem this Hamiltonian is represented in a basis a_α , $\{|\Delta\Sigma I\Sigma I, \Omega_F FM_F\rangle\}$, by a 10×10 matrix and this was diagonalized numerically using trial parameters.

The same results are obtained if one uses a Hamiltonian in a basis a_β but with the hyperfine part of the energy introduced as a perturbation in first order [Eq. (1)]. The results show that the $R(1)$ line of ${}^3\Phi_2 - {}^3\Delta_1$ for example, contains only the three "classical" hyperfine components and, thus, this possibility cannot be correct.

B. Λ perturbation

The two first components of the $R(1)$ line of the ${}^3\Phi_2 - {}^3\Delta_1$ subband appear as doublets and it is possible to envisage them as being caused by a localized perturbation removing the Λ degeneracy of the levels of the ${}^3\Delta_1$ substate. One such effect is produced by the matrix elements connecting the wavefunctions $|\Delta\Sigma I\Omega JF\rangle$ and $\sigma_v|\Delta\Sigma I\Omega JF\rangle = \epsilon|-\Delta\Sigma - \Sigma I - \Omega JF\rangle$ in the a_β basis, where σ_v is the symmetry operator for reflection in the plane xOz in the molecular frame and ϵ is a phase factor.¹⁹ After symmetrization, in the Kronig sense, of these functions, i. e.,

$$|\Delta\Sigma I\Omega JF \pm\rangle = 1/\sqrt{2}[\Delta\Sigma I\Omega JF \pm \sigma_v|\Delta\Sigma I\Omega JF\rangle]. \quad (3)$$

The matrix element of the Hamiltonian in the new basis can be written

$$\begin{aligned} \langle \Lambda' S' \Sigma' I' \Omega' J' F' \pm | H | \Delta\Sigma I\Omega JF \pm \rangle \\ = \langle \Lambda' S' \Sigma' I' \Omega' J' F' \pm | H | \Delta\Sigma I\Omega JF \rangle \\ \pm \langle \Lambda' S' \Sigma' I' \Omega' J' F' \pm | H \sigma_v | \Delta\Sigma I\Omega JF \rangle. \end{aligned} \quad (4)$$

In the particular case of the ${}^3\Delta$ state ($\Lambda = 2$), the second term on the right hand side, which will remove the Λ degeneracy, can be obtained in fourth order of perturbation theory if one uses elements with $\Delta\Lambda = \pm 1$ of the classical spin-orbit and rotational Hamiltonian, or to second order with the elements $\Delta\Lambda = \pm 2$ of the hyperfine Hamiltonian.¹

In the first case it is a substate, ${}^3\Pi_0$, ${}^3\Pi_1$, or ${}^1\Pi_1$, which perturbs the ${}^3\Delta_1$ substate in a resonant manner, and the Λ doubling term takes the form

$$\pm [\rho/(E_\Delta - E_\Pi)^2] J(J+1). \quad (5)$$

In the second case, ${}^3\Delta_1$ is perturbed by a ${}^3\Sigma$ state, any ${}^1\Sigma$ state yielding a zero matrix element. Bearing in mind the noncrossing rule, this ${}^3\Sigma$ state can only be assigned as $(5s\sigma, 4d\sigma) {}^3\Sigma$ and, since the configuration contains an s electron, it will almost certainly possess a significant hyperfine interaction. Of all the possibilities, only that one corresponding to the perturbation of the J level of the ${}^3\Delta_1$ substate by the level $N_E = J$, $J_E = J+1$ of the ${}^3\Sigma$ state would give a numerical correct agreement. The Λ doubling term then becomes

$$\pm \frac{1}{E_\Delta - E_\Sigma} \times \left[\delta^2 \frac{J(F+I+J+2)(I+J-F+1)(F+J-I+1)(F+I-J)}{2(2J+1)(2J+3)^2} \right]. \quad (6)$$

The details of this calculation will be given later.²¹ In these two cases, ρ and δ are adjustable parameters. To interpret the variation in J and F of the resonant effect, E_Δ , E_Π , and E_Σ are replaced by their total energies (including both rotational and hyperfine parts) of the corresponding states. This procedure introduces formally adjustable parameters such as, for example, the difference $B_\Delta - D_\Pi$, since the actual values are not known.

It is important to note that, if this theoretical approach is correct for lines with $J=2$, for which the resonance is not too strong, some reservations must be expressed with respect to the application of this perturbation approach to a component such as $F = \frac{9}{2}$ of $R(1)$ for which, in the second case for example, the energy difference in the denominator is only double that of the square root of the factor in brackets. In such cases, perturbation theory cannot be used in view of extensive mixing of the "perturbed" and "perturbing" states. However, in the complete absence of information about the perturbing state and with the relatively small amount of information available from the optical spectrum, such a calculation can give some idea of the relative disposition of the levels. The major arguments which decide the issue are, however, of a qualitative nature and do not, therefore, depend upon small quantitative discrepancies between theory and experiment.

In spite of these fundamental reservations, the results obtained are relatively good. For example, we give in Fig. 2 the positions²² and theoretical intensities²³ compared with the experimental observations for the case of a hyperfine perturbation with $\Delta\Lambda = 2$ by a ${}^3\Sigma$ state. The apparently good fit is, unfortunately, weakened by a large number of unfavorable arguments.

First of all is the complexity of the model and the high order of perturbation theory which one is obliged to invoke.

Second, is the fact that in each case the presence of an electronic state very close to the ${}^3\Delta$ state and, perhaps, even *below* the latter, which has been found to be, most likely, the ground state of NbN. This problem is very difficult to overcome, particularly in view of the known disposition of electronic states for the iso-electronic molecule ZrO.²⁴

Third, the lambda doubling being symmetrical, the centers of the doublets should theoretically follow a Landé interval form and this is not found experimentally.

Fourth, the two lambda components must, theoretically, have the same intensity (see Appendix). This does not appear to be true from an examination of the experimental results even though, taking into account the low intensities of these components, it is possible

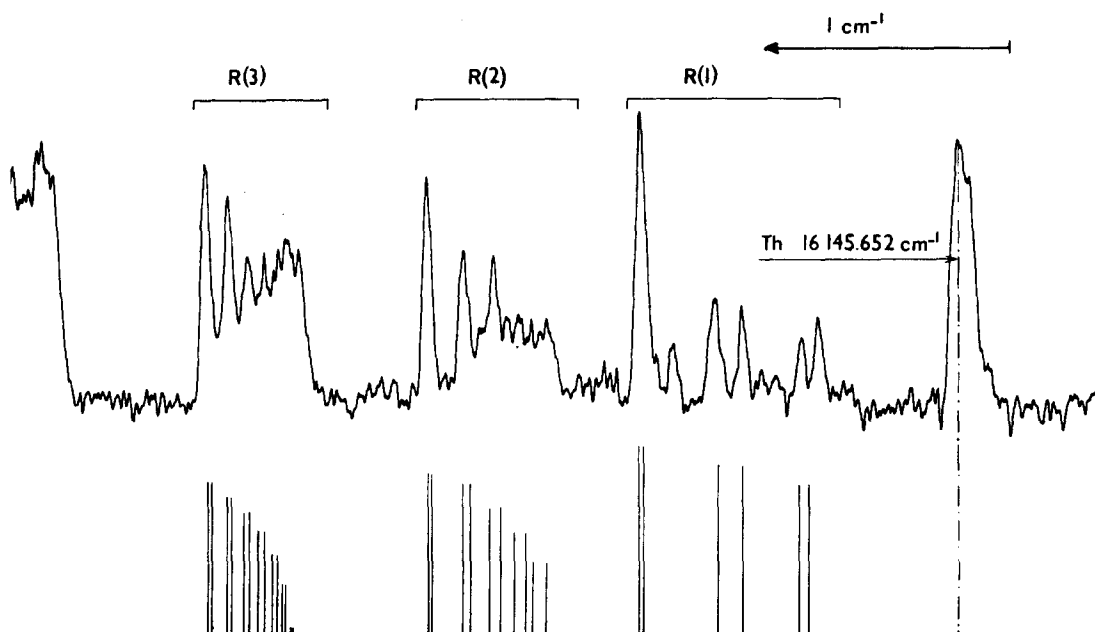


FIG. 2. Comparison of calculated and observed lines for the case of a perturbation in the ${}^3\Delta_1$ substate by a state ($\Delta\Lambda = \pm 2$).

to have some reservations about the accuracy of the photographic process in such cases.

Fifth, in order to correctly reproduce the linewidths for the ${}^3\Phi_4 \rightarrow {}^3\Delta_3$ subband lines, it is necessary to use a negative value for the "a" hyperfine parameter pertinent to the ${}^3\Delta$ state. This is incompatible with the definition¹ of

$$a = 2g_I \mu_0 \mu_\pi \langle 1/r_1^3 \rangle.$$

Sixth, and finally, we wish to point out that the differences $B_\Pi - B_\Delta$ and/or $B_C - B_\Delta$ which must be used to obtain agreement with experiment, are far too large to be reasonable (+0.075 and +0.120 cm^{-1} , respectively).

Thus, despite the plausibility of this hypothesis, we have been led to reject it as the cause of the secondary hyperfine effects.

C. Hyperfine structure in the ${}^3\Phi$ state

The necessity for a negative a_Δ value in the preceding model led us to investigate the effect of a nonnegligible value of a_Φ , i. e., in the excited state. As a first approximation this was done by considering $a_\Delta \sim 0$ and $b_\Phi + c_\Phi \sim 0$, i. e., we assumed

$$(b_\Delta + c_\Delta) \Sigma [\Omega/J(J+1)] \mathbf{I} \cdot \mathbf{J}, \quad (7)$$

and

$$a_\Phi \Lambda [\Omega/J(J+1)] \mathbf{I} \cdot \mathbf{J}, \quad (8)$$

to give the hyperfine corrections to the lower and upper states, respectively.

With these premises for each lower level $(J, F)_\Delta$ there are three transitions possible

$$(J+1, F+1)_\Phi \rightarrow (J, F)_\Delta,$$

$$(J+1, F)_\Phi \rightarrow (J, F)_\Delta,$$

$$(J+1, F-1)_\Phi \rightarrow (J, F)_\Delta.$$

As a consequence, each hyperfine component may be split into three lines, although the spectrum itself shows only two. We have, therefore, undertaken the calculation of the intensity factors corresponding to these transitions using the techniques of the MI method.²⁰

The details of this calculation will be given elsewhere²¹ but the formulas obtained have been given in the Appendix for reference purposes. It is found that one of the components of the hyperfine triplet has a very low intensity and that the other two have intensities in agreement with the experimental observations.

On obtaining spectra of better resolution and reciprocal dispersion, it became necessary to improve the original postulates by introducing the more general case where $a_\Delta \neq 0$ and $(b_\Phi + c_\Phi) \neq 0$. We have, then, been able to calculate the positions (and intensities) of the hyperfine components using the pair of expressions

$$H_\Phi = T_{0\Phi} + B_\Phi J(J+1) + H_{\text{hfs}}, \quad (9)$$

$$H_\Delta = T_{0\Delta} + B_\Delta J(J+1) + H_{\text{hfs}},$$

for each subband observed in the spectrum, i. e., three in all. The terms which are off diagonal in Σ or in Λ have been ignored since they will be unimportant in the first few lines studied in each subband. They will, however, be taken into account in a subsequent study¹⁸ of the fine structure of the ${}^3\Phi \rightarrow {}^3\Delta$ transition of NbN.

The results obtained are given in the conventional form of bars in Figs. 1.²⁵

The excellent agreement between theory and experiment in this case strongly suggests this as the correct model for the secondary hyperfine effects observed.

TABLE I. Best values of one-electron parameters a and $b+c$ as obtained for both Δ and Φ states (in cm^{-1}).

Parameter	State	
	Φ	Δ
a	0.017 ± 0.003	0.016 ± 0.0003
$b+c$	-0.011 ± 0.007	0.098 ± 0.005

IV. NUMERICAL RESULTS

In the calculation of the frequencies by the use of formulas (9) we have used the values of B_Δ and B_Φ which have been deduced¹⁸ from a study of the fine structure of the ${}^3\Phi - {}^3\Delta$ system of NbN.

As far as the hyperfine parameters are concerned, only a very small number of single lines can be assigned with complete confidence—particularly in the subband ${}^3\Phi_4 - {}^3\Delta_3$ —so that the method of least squares is not valid. It is possible that a further experimental study using interferometry might be useful in this matter. However, because of the high quality of the information obtained from the ${}^3\Phi_2 - {}^3\Delta_1$ subband, we have been able to obtain good values for the quantities $3a_\Phi - (b_\Phi + c_\Phi)$ and $2a_\Delta - (b_\Delta + c_\Delta)$, and these have been used to reproduce the actual spectrum in a very satisfactory way (see Fig. 1). Overlapping of the most “instructive” lines in the ${}^3\Phi_4 - {}^3\Delta_3$ subband has made the determination of the quantities $3a_\Phi + (b_\Phi + c_\Phi)$ and $2a_\Delta + (b_\Delta + c_\Delta)$ a less precise situation. In this latter case, the information obtained from the *linewidths* has been used to confirm the results. The best values are given in Table I.

The errors have been estimated from the differences between the values obtained for the four effective constants $3a_\Phi \pm (b_\Phi + c_\Phi)$ and $2a_\Delta \pm (b_\Delta + c_\Delta)$. It is also of note that only the sums $b_\Phi + c_\Phi$ and $b_\Delta + c_\Delta$ could be obtained from our analysis.

V. DISCUSSION

A. The ${}^3\Delta$ state

The most important cause of the hyperfine effects observed in the rotational levels of the ${}^3\Delta$ state of the NbN molecule is clearly the Fermi contact term $bI \cdot S$ in Frosch and Foley's hyperfine Hamiltonian.¹ They pointed out the significance of the parameter b as an indication of the presence of s electron density and this was the reason for the original assignment¹⁷ of the ${}^3\Delta$ (probably the ground) state of NbN as arising from the configuration ($5s\sigma$, $4d\delta$) essentially localized on the niobium atom.

As an initial approximation the wavefunctions appropriate to the ${}^3\Delta_1$ and ${}^3\Delta_3$ substates can be represented by the tensor products of the one electron functions $|\sigma\beta, d\delta\beta\rangle$ and $|\sigma\alpha, d\delta\alpha\rangle$, respectively. These functions are actually atomic wavefunctions centered on the metal ion as is usual in this kind of molecule.^{26,13} With this approximation and using the fact that $c=0$ when the

charge distribution is spherical, a rough calculation shows that the effective parameters deduced in the preceding section, can be related to the one electron parameters by the following:

$$a_\Delta \sim 2a_\delta, \\ b_\Delta + c_\Delta = \frac{1}{2}(b_\sigma + b_\delta + c_\delta) \sim \frac{1}{2}b_\sigma - b_\delta. \quad (10)$$

The last expression follows if one takes account of the relation $c_\delta \sim -3b_\delta$ in the absence of any s electron contribution. It is clear that b_δ is very small compared with b_σ . This arises from the form of b ,¹ i. e.,

$$b = 2g_I \mu_0 \mu_n \left[\frac{2}{3} \cdot \frac{\delta(r_1)}{r_1^2} - \frac{3 \cos^2 \chi - 1}{2r_1^3} \right]_{av},$$

and the fact that $|d\delta\rangle \rightarrow 0$ as $r_1 \rightarrow 0$ while $|\sigma\rangle$ does not. In this case, a one electron parameter b_σ , can be obtained, i. e., $b_\sigma({}^3\Delta, \text{NbN}) = 2 \times 0.098 = 0.196 \text{ cm}^{-1}$. The same type of analysis may be applied to the hyperfine effects observed⁵ in the transition ${}^4\Pi - {}^4\Sigma$ and ${}^4\Sigma - {}^4\Sigma$ of NbO and the formulas for the hypermultiplet widths derived by one of us previously⁵ can be used to obtain an effective parameter $b \sim 0.064 \text{ cm}^{-1}$.

If it is assumed that this structure is *completely* localized in the ground ${}^4\Sigma^-(b_{\beta,r})$ state of NbO, bearing in mind that the open shell contains only a single s contribution, and using a rough calculation similar to that employed by Richards and Barrow,¹² we obtain for the one electron parameter b_σ :

$$b_\sigma({}^4\Sigma, \text{NbO}) \sim 3 \times 0.064 = 0.192 \text{ cm}^{-1},$$

which is almost identical with the value obtained for the NbN ${}^3\Delta$ state.

These results confirm that in both the ${}^3\Delta$ state of NbN and the ${}^4\Sigma^-$ state of NbO, the hyperfine effect is essentially due to the contribution of an s type electron and that this contribution varies very little from the nitride to the oxide—surely a surprising conclusion if the conventional concepts of the electronic contribution to the binding energy of such molecules are espoused.

B. The ${}^3\Phi$ state

This state appears to be, what will probably turn out to be rare, an example of an excited state with case a_β hyperfine coupling. In fact, except for the example of HgH,^{2,3} where the hyperfine structure of the $A_1 {}^2\Pi_{1/2}$ state owes its appearance entirely to an abnormal Λ doubling effect, other examples of this type (a_β) are either complicated by quadrupolar effects (e. g. InH⁵), which is insignificant for NbN due to the very small value of Q for Nb,⁵ or else show strong case c tendencies (e. g. BiH^{4,5} and InH²⁷). This latter problem has been underscored in the case of the ${}^3\Pi$ state of InH where the case c tendency is necessary to explain the presence of hyperfine effects in the center subband where the zero value of Σ causes the important hyperfine terms to vanish in case a_β .

This effect, suggested in II as a possible explanation of the linewidth of the $R(2)$ line in the ${}^3\Phi_3 - {}^3\Delta_2$ subband is not really necessary as reference to Fig. 1 (b) shows.

What at first sight appears as a large width of the $R(2)$ line in a weak spectrum, is seen in a much more intense spectrum as due to the presence of a line which is not a part of the structure of this subband. This eliminates any necessity for invoking case c tendencies in NbN. A calculation analogous to that carried out for the ${}^3\Delta$ state and using the simplified wavefunctions $|p\pi\beta, d\delta\beta\rangle$ for ${}^3\Phi_2$ and $|p\pi\alpha, d\delta\alpha\rangle$ for ${}^3\Phi_4$ once again allows us to express the observed "term" parameters as one electron parameters. In particular,

$$a_\Phi \sim a_\tau + 2a_\delta, \\ b_{\Phi+} + c_{\Phi-} \sim b_\tau - b_\delta \quad (\text{with } c_\tau = -3b_\tau \text{ and } c_\delta = -3b_\delta), \quad (11)$$

and taking into account the result found previously, i. e., that $a_\Phi \sim a_\Delta$, a comparison of the relations (10) and (11) suggests that $a_\tau \ll a_\delta$ the latter having the value 0.008 cm^{-1} . This strongly suggests that it is the $4d\delta$ electron which is responsible for the hyperfine structure observed for the ${}^3\Phi$ state, its contribution in the ${}^3\Delta$ state being effectively masked by the much larger b_Δ contribution from the $5s\sigma$ electron. This, in turn, suggests that a similar contribution from the a term is unlikely to be observed in the $(d\delta^2, p\sigma) {}^4\Sigma^-$ and $(d\sigma^2, p\pi) {}^4\Pi$ excited states of NbO since, in these examples, the l_z components (along the internuclear axis) of the one electron orbital moments l of the two $d\delta$ electrons, are opposite to one another and their individual hyperfine contributions, $al_z I_z$, cancel identically.

APPENDIX

The intensity factors used in this paper were calculated using the MI method which has been discussed more completely elsewhere.^{20,21} In the particular case of a transition of a molecule with coupling a_b , for which $\Omega' = \Omega + 1$, to a state also with coupling a_b , the intensity factors are as follows:

$$\begin{aligned} R \text{ branch} & \quad J' = J + 1 \rightarrow J \\ F' = F + 1 \rightarrow F & \quad g_R(\Omega, J) \times \frac{(I + J + F + 2)(I + J + F + 3)(J + F - I + 1)(J + F - I + 2)}{F + 1} \\ F' = F \rightarrow F & \quad g_R(\Omega, J) \times \frac{(I + J + F + 2)(F + J - I + 1)(I + J - F + 1)(I + F - J)(2F + 1)}{F(F + 1)} \\ F' = F - 1 \rightarrow F & \quad g_R(\Omega, J) \times \frac{(I + J - F + 1)(I + J - F + 2)(I + F - J - 1)(I + F - J)}{F}, \end{aligned}$$

where

$$g_R(\Omega, J) = \frac{(J + \Omega + 1)(J + \Omega + 2)}{8(J + 1)^2(2J + 1)(2J + 3)}$$

$$\begin{aligned} Q \text{ branch} & \quad J' = J \rightarrow J \\ F' = F + 1 \rightarrow F & \quad g_Q(\Omega, J) \frac{(I + J + F + 2)(J + F - I + 1)(I + F - J + 1)(I + J - F)}{F + 1} \\ F' = F \rightarrow F & \quad g_Q(\Omega, J) \frac{[J(J + 1) + F(F + 1) - I(I + 1)]^2(2F + 1)}{F(F + 1)} \\ F' = F - 1 \rightarrow F & \quad g_Q(\Omega, J) \frac{(I + J + F + 1)(J + F - I)(I + F - J)(I + J - F + 1)}{F}, \end{aligned}$$

where

$$g_Q(\Omega, J) = \frac{(J - \Omega)(J + \Omega + 1)}{8J^2(J + 1)^2}$$

$$P \text{ branch} \quad J' = J - 1 \rightarrow J$$

VI. CONCLUSIONS

After consideration of the possible origins for the secondary hyperfine effect in the $(0, 0)$ band of the ${}^3\Phi \rightarrow {}^3\Delta$ system of NbN, the most satisfactory explanation is that of a nonnegligible hyperfine effect on the ${}^3\Phi$ state. Analysis of spectra obtained at an even higher dispersion and resolving power than were used previously,¹⁷ coupled with a theoretical study of the hyperfine transition intensities, has confirmed this hypothesis.

The complete analysis of the rotational fine structure of this system is presently under way. This study has revealed the existence of an "anomalously" large linewidth in the region of high J ($\gtrsim 50$) in the ${}^3\Delta_1$ state which could be due either to Λ doubling in the ${}^3\Delta$ state or, perhaps even more interestingly, a further hyperfine effect resulting from a decoupling of the electron spin in one of the two states, with the resultant transition from case a_b towards b_{bJ} nuclear coupling. The presence of a perturbation appears to be unlikely.

ACKNOWLEDGMENTS

This work was supported by the National Science Foundation Grant No. GP 16089 to one of us (T. M. D.). C. A. and J. -L. F. also wish to acknowledge the support provided by the National Science Foundation and the hospitality of the Chemistry Department of the University of Michigan at Ann Arbor.

$$F' = F + 1 \rightarrow F \quad g_P(\Omega, J) \frac{(I+J-F-1)(I+J-F)(I+F-J+1)(I+F-J+2)}{F+1}$$

$$F' = F \rightarrow F \quad g_P(\Omega, J) \frac{(I+F+J+1)(F+J-I)(I+J-F)(I+F-J+1)(2F+1)}{F(F+1)}$$

$$F' = F - 1 \rightarrow F \quad g_P(\Omega, J) \frac{(I+F+J)(I+F+J+1)(F+J-I-1)(F+J-I)}{F} ,$$

where

$$g_P(\Omega, J) = \frac{(J-\Omega-1)(J-\Omega)}{8J^2(2J+1)(2J-1)}$$

These factors were used in the model described in III. C. For the model described in III. B which implies the presence of lambda doubling, each component of an F doublet is obtained by the superposition of three hyperfine components

$$F' = F + 1 \rightarrow F, \quad F' = F \rightarrow F, \quad \text{and} \quad F' = F - 1 \rightarrow F .$$

The second of those three intensity factors yields the following simplified formulas

$$R \text{ branch} \quad \frac{(J+\Omega+1)(J+\Omega+2)}{2(J+1)(2J+1)} (2F+1) ,$$

$$Q \text{ branch} \quad \frac{(J-\Omega)(J+\Omega+1)}{2J(J+1)} (2F+1) ,$$

$$P \text{ branch} \quad \frac{(J-\Omega)(J-\Omega-1)}{2J(2J+1)} (2F+1) .$$

*Present address: Laboratoire d'Optique Atomique et Moléculaire, Faculté des Sciences S. P. C. N. I., Parc Valrose, 06034 Nice Cedex, France.

¹R. A. Frosch and H. M. Foley, Phys. Rev. 88, 1337 (1952).

²T. L. Porter and S. P. Davis, J. Opt. Soc. Am. 53, 338 (1963).

³D. M. Eakin and S. P. Davis, J. Mol. Spectrosc. 35, 27 (1970).

⁴E. Hulthén and H. Neuhaus, Phys. Rev. 102, 1415 (1956).

⁵T. M. Dunn, in *Molecular Spectroscopy: Modern Research*, edited by Rao and Mathews (Academic, New York, 1972), Ch. 4.4.

⁶H. E. Radford, Phys. Rev. A 136, 1571 (1964).

⁷K. M. Evenson, J. L. Dunn, and H. P. Broida, Phys. Rev. A 136, 1566 (1964).

⁸R. L. Barger, H. P. Broida, A. J. Estlin, and H. E. Radford, Phys. Rev. Lett. 9, 345 (1962).

⁹R. F. Barrow, W. J. M. Gissane, and R. Richards, Proc. R. Soc. A 300, 469 (1967).

¹⁰P. W. Atkins, Proc. R. Soc. A 300, 487 (1967).

¹¹D. Richards and R. F. Barrow, Nature (Lond.) 217, 842 (1968).

¹²D. Richards and R. F. Barrow, Nature (Lond.) 219, 1244 (1968).

¹³A. Adams, W. Klemperer, and T. M. Dunn, Can. J. Phys. 46, 2213 (1968).

¹⁴R. Stringat, C. Athénour, and J.-L. Féménias, Can. J. Phys. 50, 395 (1972).

¹⁵R. Bacis and A. Bernard, Can. J. Phys. 51, 648 (1973).

¹⁶R. Bacis, N. Bessis, and R. Collomb, Phys. Rev. A 8, 2255

(1973).

¹⁷T. M. Dunn and K. M. Rao, Nature (Lond.) 222, 266 (1969).

¹⁸Further details will be given in a paper to be submitted elsewhere on the analysis of the fine structure of NbN by C.

Athénour, T. M. Dunn, J.-L. Féménias, and K. M. Rao.

¹⁹J. T. Hougen, Monogr. U.S. Natl. Bur. Stand. 115 (1970).

²⁰J.-L. Féménias, C. Athénour, and R. Stringat, Can. J. Phys. 52, 361 (1974).

²¹J.-L. Féménias and C. Athénour (to be published). Can. J. Phys.

²²The positions were calculated approximating the Hamiltonian for the $^3\Phi_2$ state by $T_{0\Phi} + B_{\Phi_2} J(J+1)$, while that for the $^3\Delta_1$ was $T_{0\Delta_1} + B_{\Delta_1} J(J+1) + H_{\text{hts}} \pm H_{\Lambda\text{doub}}$. These approximations are sufficient for a study of the five first lines in each sub-state.

²³The theoretical densities are given in the Appendix and, see also, Ref. 25.

²⁴L. Brewer and D. W. Green, High Temp. Sci. 1, 26 (1969).

²⁵The experimental densities are of the form $d = \alpha \log It + \beta'$ where t is the exposure time and I is the intensity, proportional to the Boltzman factor which depends upon J and on the intensity factor f , calculated in the Appendix. The Boltzman factor is almost constant over the range of our study and we may then write $d = \alpha \log f + \beta$. To take the response of the plate into account, the lowest intensity lines were not measured. Their positions are indicated by ●. For the other lines, the bar height is proportional to $\log f$.

²⁶K. D. Carlson, E. Ludenā, and C. Moser, J. Chem. Phys. 43, 2408 (1965).

²⁷K. F. Freed, J. Chem. Phys. 45, 1714 (1966).